

Unclassified

1

DOCUMENTATION PAGE

Form Approved  
OMB No. 0704-0188

AD-A220 966

2b. DECLASSIFICATION/DOWNGRADING SCHEDULE  
APR 24 1990

4. PERFORMING ORGANIZATION REPORT NUMBER(S)

GL-TR-90-0076

6a. NAME OF PERFORMING ORGANIZATION

Geophysics Laboratory (AFSC)

6b. OFFICE SYMBOL  
(if applicable)

GL(OPI)

1b. RESTRICTIVE MARKINGS

3. DISTRIBUTION/AVAILABILITY OF REPORT

Approved for public release;  
Distribution unlimited

5. MONITORING ORGANIZATION REPORT NUMBER(S)

6c. ADDRESS (City, State, and ZIP Code)

Hanscom AFB  
Massachusetts 01731-5000

7a. NAME OF MONITORING ORGANIZATION

8a. NAME OF FUNDING/SPONSORING  
ORGANIZATION

8b. OFFICE SYMBOL  
(if applicable)

9. PROCUREMENT INSTRUMENT IDENTIFICATION NUMBER

8c. ADDRESS (City, State, and ZIP Code)

10. SOURCE OF FUNDING NUMBERS

PROGRAM ELEMENT NO	PROJECT NO	TASK NO	WORK UNIT ACCESSION NO
61102F	2310	G4	23

11. TITLE (Include Security Classification)

The Radiative Lifetime of  $N_2(a^1\Pi_g, v=0-2)$

12. PERSONAL AUTHOR(S) William J. Marinelli\*, William J. Kessler\*, Byron David Green\*,  
and William A. M. Blumberg

13a. TYPE OF REPORT  
Reprint

13b. TIME COVERED  
FROM \_\_\_\_\_ TO \_\_\_\_\_

14. DATE OF REPORT (Year, Month, Day)  
1990 April 3

15. PAGE COUNT  
7

16. SUPPLEMENTARY NOTATION

\* Physical Sciences Inc., Research Park, Andover, MA 01810  
Reprinted from the Journal of Chemical Physics, Vol. 91, p. 701 (1989)

17. COSATI CODES

FIELD	GROUP	SUB-GROUP

18. SUBJECT TERMS (Continue on reverse if necessary and identify by block number)

Nitrogen Lyman-Birge-Hopfield Bands; Radiative  
Lifetimes;  $N_2(a^1\Pi_g)$  State

19. ABSTRACT (Continue on reverse if necessary and identify by block number)

We have employed direct two-photon laser excitation of specific vibrational levels of  $N_2(a^1\Pi_g)$  to measure the lifetime of this state. Direct observation of emission from the  $a^1\Pi_g-X^1\Sigma_g^+$  transition in a large cell was employed to follow fluorescence decays. Experiments were conducted to verify that the effects of collisional transfer and diffusion were not contributing to the observed lifetime. Our experiments showed that the radiative lifetime of vibrational levels 0-2 is  $56 \pm 4 \mu s$  and is independent of vibrational level, within experimental error. The observed lifetimes are in good agreement with recently reported theoretical calculations.

20. DISTRIBUTION/AVAILABILITY OF ABSTRACT

☐ UNCLASSIFIED/UNLIMITED ☒ SAME AS RPT ☐ DTIC USERS

21. ABSTRACT SECURITY CLASSIFICATION

Unclassified

22a. NAME OF RESPONSIBLE INDIVIDUAL

William A.M. Blumberg

22b. TELEPHONE (Include Area Code)

(617)377-2810

22c. OFFICE SYMBOL

GL(AFSC)/OPI

# The radiative lifetime of $N_2(a^1\Pi_g, v=0-2)$

William J. Marinelli, William J. Kessler, and Byron David Green  
Physical Sciences Inc., Research Park, P.O. Box 3100, Andover, Massachusetts 01810

William A. M. Blumberg  
Air Force Geophysics Laboratory, Hanscom Air Force Base, Massachusetts 01731

(Received 1 March 1989; accepted 6 April 1989)

We have employed direct two-photon laser excitation of specific vibrational levels of  $N_2(a^1\Pi_g)$  to measure the lifetime of this state. Direct observation of emission from the  $a^1\Pi_g-X^1\Sigma_g^+$  transition in a large cell was employed to follow fluorescence decays. Experiments were conducted to verify that the effects of collisional transfer and diffusion were not contributing to the observed lifetime. Our experiments showed that the radiative lifetime of vibrational levels 0-2 is  $56 \pm 4 \mu s$  and is independent of vibrational level, within experimental error. The observed lifetimes are in good agreement with recently reported theoretical calculations.

## INTRODUCTION

Knowledge of the radiative lifetimes of the low-lying metastable states of  $N_2$  is of great importance to our understanding of such phenomena as energy transfer processes in auroral excitation, chemical lasers, and high-voltage switching. In spite of their importance, the lifetimes of these states are still poorly known due to the experimental difficulties which arise in observing such long-lived species.

The  $a^1\Pi_g$  state of  $N_2$  is a prominent emitter in the vacuum ultraviolet (VUV) spectrum of aurorally excited  $N_2$ .<sup>1-6</sup> The  $a^1\Pi_g-X^1\Sigma_g^+$  Lyman-Birge-Hopfield (LBH) bands extend from approximately 130 to 200 nm comprising emission from  $v'=0-6$  of the  $a^1\Pi_g$  state.<sup>7</sup> Levels above  $v'=6$  undergo a weak predissociation and are not observed in emission. The LBH transition is dipole forbidden. Hence, the observed transition strength is due to contributions from the magnetic dipole and electric quadrupole moments. In addition to emission through the LBH bands, the  $a^1\Pi_g$  state may exchange radiation with the  $a'^1\Sigma_u^+$  state. The origin of this state lies  $1212 \text{ cm}^{-1}$  below the  $a^1\Pi_g$  and the nested vibrational levels of these states allow for collisional and radiative exchange of energy in this coupled system. A potential-energy level diagram of these states is shown in Fig. 1. Infrared emission from these transitions was first observed by McFarlane.<sup>8</sup> Due to the low frequency of these transitions, they may contribute only a few percent to the total radiative decay rates.

The radiative lifetime of the  $a$  state has been the subject of numerous investigations. In spite of these efforts, the reported values cover a range of over a factor of 3. Early experiments by Lichten<sup>9</sup> employed a molecular beam time-of-flight method to measure a lifetime of  $1.70 \pm 0.30 \times 10^{-4} \text{ s}$ . He used electron excitation near threshold to produce the metastable  $N_2$ . A particle detector was employed to measure the arrival time of all metastables at a fixed distance from the point of production. This detector could not discriminate between different metastable species. His analysis included production of the  $A^3\Sigma_u^+$  and  $a^1\Pi_g$  states. However, the analysis did not account for production of the  $a'^1\Sigma_u^+$  state, which was assumed to have a short lifetime. Similar experi-

ments performed by Olmstead and co-workers,<sup>10</sup> and Borst and Zipf<sup>11</sup> gave lifetimes of  $1.20 \pm 0.50 \times 10^{-4} \text{ s}$  and  $1.15 \pm 0.20 \times 10^{-4} \text{ s}$ , respectively. Neither study included radiative decay of the  $a'$  state in the analysis of their time-of-flight (TOF) data. More recent measurements by Mason and Newell,<sup>12</sup> who used a similar TOF method, support the lifetime obtained by Borst and Zipf. Additional measurements by Holland<sup>13</sup> employed a spectrometer and scanning photometer to measure the radial extent of LBH emission from a collimated electron beam traversing a low pressure ( $10^{-4} \text{ Torr}$ )  $N_2$  sample. An analysis of the emission gave an upper limit to the lifetime of  $0.80 \times 10^{-4} \text{ s}$ . The inclusion of cascade from higher levels of  $N_2$  excited by the electron beam in their model would reduce the calculated lifetime. This lifetime appears to be the most reliable of the decay measurements.

Several studies have employed absorption oscillator strength measurements on the LBH transition to infer radiative lifetimes. These measurements cannot measure any contribution to the lifetimes from other channels, such as the  $a-a'$  transition. Garstang<sup>14</sup> analyzed measurements of gen-

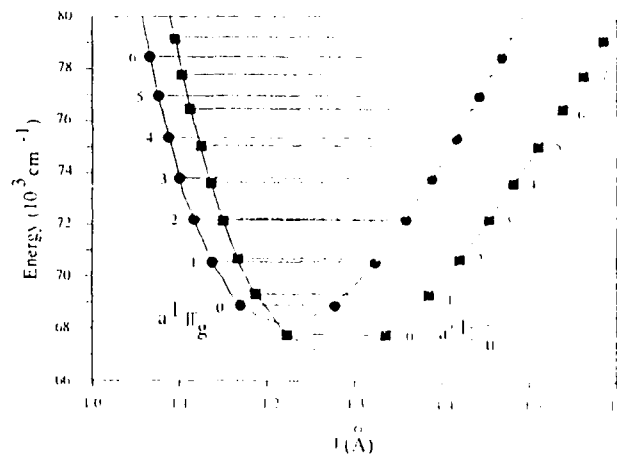


FIG. 1. Potential-energy diagram for the lowest vibrational levels of the  $N_2(a'^1\Pi_g)$  and  $N_2(a^1\Sigma_u^+)$  states.

eralized oscillator strengths to obtain a total lifetime of  $0.46 \times 10^{-4}$  s. The pressure-broadened absorption intensities of Ching and co-workers<sup>15</sup> were analyzed to give a lifetime of  $0.30 \times 10^{-4}$  s. Subsequent measurements of oscillator strengths by Shemansky<sup>16</sup> for levels 0–8 gave lifetimes ranging from  $1.4$  to  $1.6 \times 10^{-4}$  s. These measurements were later reexamined by Ajello and Shemansky<sup>17</sup> and adjusted downward to match the value measured by Holland. Pilling and co-workers<sup>18</sup> obtained lifetimes ranging from  $0.76$  to  $1.16 \times 10^{-4}$  s for levels 1–6 from their curves of growth method of determining oscillator strengths.

Recently, Dahl and Oddershede<sup>19</sup> employed a second-order polarization propagator method (SOPPA) to calculate the radiative rate of the  $a-X$  transition. They calculated radiative lifetimes ranging from  $0.59 \times 10^{-4}$  to  $0.68 \times 10^{-4}$  s for vibrational levels 0–4, respectively. Their calculation showed that the oscillator strength is derived almost solely from the magnetic dipole moment and only 4% to 5% can be attributed to the electric quadrupole moment.

The experiments which we are reporting on in this paper were carefully designed to measure the radiative lifetime of  $N_2(a)$ . Selective two-photon laser excitation of the  $N_2(a,v)$  level to be studied is employed to eliminate interference from cascade effects common to all the electron beam excitation studies. Direct detection of  $N_2(a-X)$  emission is employed. Under these conditions simple Stern-Volmer-type kinetic analysis may be utilized to extract the lifetime data for  $v' = 0$ . For vibrational levels 1 and 2 coupled relaxation with the  $a' ^1\Sigma_u$  state complicates the kinetic analysis. However, the experiments are conducted at sufficiently low pressures that collision-free lifetimes may be obtained for these levels directly from the data. The experiments reported here complement our previous studies on the coupled relaxation of the  $a-a'$  state manifold<sup>20</sup> and the quenching of  $N_2(a,v = 0)$  by several species important in auroral chemistry.<sup>21</sup>

## EXPERIMENTAL

A crucial factor in the design of experiments to measure lifetimes of long-lived species is the avoidance of field-of-view (FOV) and wall effects. The treatment of such measurements was described in detail by Sackett.<sup>22</sup> The species must be produced sufficiently far from the fluorescence cell walls such that transport to the walls does not result in significant heterogeneous deactivation. Similarly, thermal motion of molecules out of the detector field of view must be limited to a rate much less than the radiative rate. If either of these conditions is not satisfied, the effective loss rate measured experimentally includes a transport contribution and thus the experiment overestimates the radiative rate. The practical consequence of these considerations is that the time required to leave the field of view, in the collision free regime, should be no less than about 4 radiative lifetimes. Of course, the cell walls should lie outside or define the field of view. Since few molecules will leave the FOV during the early decay times, analysis of the decay profiles for the initial part of the decay minimizes errors due to FOV effects. This consideration is somewhat mitigated by the weighting accorded points at early times (maximum intensity) in the least-squares fit used to determine the decay rate. An analysis of

our experimental configuration similar to the analysis described by Sackett indicates that the measured lifetime can be no greater than 5% below the actual value. This analysis was confirmed by experiments which will be described below.

In our experiments a large steel cross was used as the fluorescence chamber. The inner diameter of the cross was 20 cm. Two additional arms, located normal to the plane of the cross, were employed to introduce light from the excitation laser. A schematic diagram of the excitation cell is shown in Fig. 2. Fluorescence from  $N_2(a)$  was detected using a solar-blind PMT (EMR-542G-17, CSI photocathode) located on the center axis of one arm of the cross. The PMT has a 28.7 mm effective diameter photocathode. The FOV of the cathode was apertured to insure that it met the walls at the point where the laser beam enters the chamber. The excitation laser is focussed using a 12.5 cm focal length lens located in the baffle arm. The light is recaptured by a baffle arm on the opposite side of the chamber, which is equipped with a Brewster-angle window and Wood's horn. Since excitation of  $N_2(a)$  is a two-photon process, it is preferentially produced in the small confocal volume of the lens in the center of the chamber. In the low-pressure limit, where the mean free path of an  $N_2$  molecule is larger than the distance from the center of the chamber to the nearest wall, transit to the wall requires approximately  $220 \mu\text{s}$  at thermal velocities. If the  $N_2(a)$  lifetime is near  $80 \mu\text{s}$ , as previous measurements would suggest, greater than 94% of the excited state molecules produced by the laser would radiate prior to leaving the detector FOV. Since the detection volume is defined by an extended cylinder, the use of the cylinder radius in our calculation is quite conservative.

A frequency doubled Nd:YAG pumped tunable dye laser was employed to excite  $N_2(a,v)$  in the experiments. Energies from 10–20 mJ per pulse at a repetition rate of 10 Hz

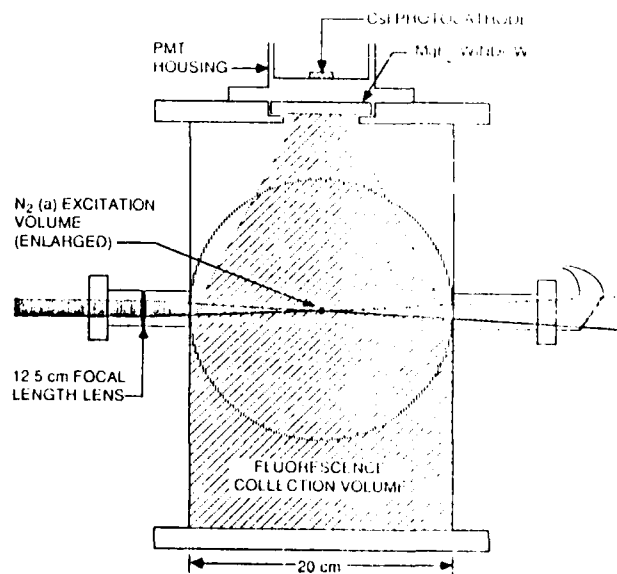


FIG. 2. Schematic diagram of the fluorescence cell used for the lifetime measurements. The approximate detector field of view is indicated by the shaded region.

were obtained from the laser. The location of the  $N_2(v' = 0)$  bands excited by the laser in these experiments were measured experimentally using 2 + 2 REMPI spectroscopy on the  $a-X$  bands in a small discharge flow reactor. The excitation laser wavelength was set to excite the  $S$  branch band head ( $J = 6-8$ ) for all the transitions studied. No effort was made to determine the lifetime as a function of rotational level. The levels studied are too low in energy to be effected by predissociation and no perturbations have been reported for this system.<sup>7</sup> The solar-blind PMT was operated in photon counting mode. A multichannel scaler was employed to count the photon pulses as a function of time following the laser pulse. A dwell time of 2  $\mu$ s/channel was used in all experiments. Typically 8000 channels of data were recorded for each pulse and data from 10 000 laser shots was averaged to obtain a single decay profile. The PMT was separated from the chamber by a 2 mm diam  $MgF_2$  window. The housing was purged with high flows of dry  $N_2$  to eliminate VUV absorption by atmospheric  $O_2$ .

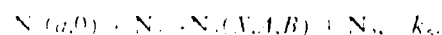
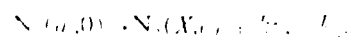
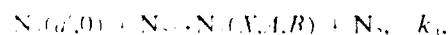
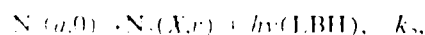
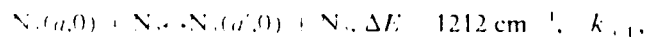
The fluorescence chamber was internally blackened using a low vapor pressure solar absorbing black paint (3M ECP-2200) to minimize scattered light. The chamber was pumped by a cryotrapped 8 in. diam diffusion pump with an effective pumping speed of 1500  $l s^{-1}$ . The blank-off pressure of the chamber was less than  $10^{-6}$  Torr. Reagent grade  $N_2$  at pressures from 0.1 to 80 mTorr ( $3.3 \times 10^{12}$  to  $2.6 \times 10^{15}$  molecules  $cm^{-3}$ ) was used for these experiments. At the higher pressures the diffusion pump was throttled using a gate valve. Typical gas flow rates of 10  $\mu$ mol  $s^{-1}$  were employed. Pressure in the chamber was measured using a high accuracy 0 to 1 Torr capacitance manometer (MKS Instruments).

## RESULTS

Experiments were conducted to measure the lifetimes of  $v' = 0, 2$  of the  $a$  state. However, the kinetics of determining the lifetimes of levels 1 and 2 are complicated by the presence of resonant energy exchange between the  $a$  and  $a'$  states. We will first discuss the measurements of the lifetime of  $v' = 0$  and then address the lifetimes of the higher levels.

### A. Vibrational level 0

The relaxation of  $v' = 0$  in  $N_2$  is described by the reaction sequence



If  $N_2(a, 0)$  is produced on a time scale fast compared to the relaxation rates, we have previously shown<sup>21</sup> that the decay of this state is given by the equation

$$[N_2(a, t)] = [N_2(a)]_0 \left[ \frac{(\lambda_2 - C_{11})}{\lambda_2 - \lambda_1} e^{-\lambda_2 t} + \frac{(C_{11} - \lambda_1)}{\lambda_2 - \lambda_1} e^{-\lambda_1 t} \right],$$

where  $C_{11} = (k_1 + k_5)[N_2] + k_2$  and  $\lambda_1$  and  $\lambda_2$  are to a good approximation given by

$$\lambda_1 = (k_1 + k_5)[N_2] + k_2, \quad \lambda_2 = (k_1 + k_3)[N_2] + k_4.$$

Thus,  $\lambda_1$  describes the initial decay of  $N_2(a, 0)$  through both collisional ( $k_1 + k_5$ ) and radiative ( $k_2$ ) processes. The rate  $\lambda_2$  describes the decay of the system from the coupled equilibrium achieved at higher pressures and longer times. Thus, at low pressures the decay of  $N_2(a, 0)$  should appear as a single exponential function. At higher pressures the decay should appear biexponential, showing the initial decay to a coupled equilibrium and the subsequent decay of the coupled system. Thus, by fitting the decay data to a single exponential at low pressure or a biexponential at higher pressures the value of  $\lambda_1$  may be determined. A plot of  $\lambda_1$  vs  $N_2$  number density should give  $k_1 + k_5$  as the slope and  $k_2$ , the radiative rate of interest, as the intercept.

The decay of  $N_2(a, 0)$  as a function of time is shown at pressures of 0.9 and 50 mTorr ( $3.0 \times 10^{13}$  and  $1.6 \times 10^{15}$  molecules  $cm^{-3}$ ) in Fig. 3. At 0.9 mTorr the mean free path of  $N_2$  is comparable to the chamber dimensions and only a single exponential decay is observed. At 50 mTorr collisional equilibrium is fully established with the  $a'$  state and a double

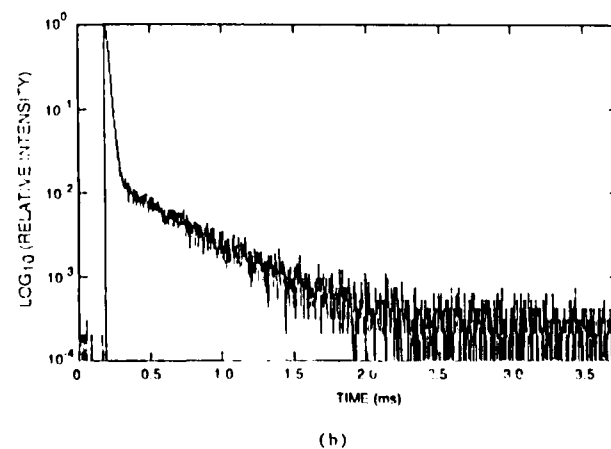
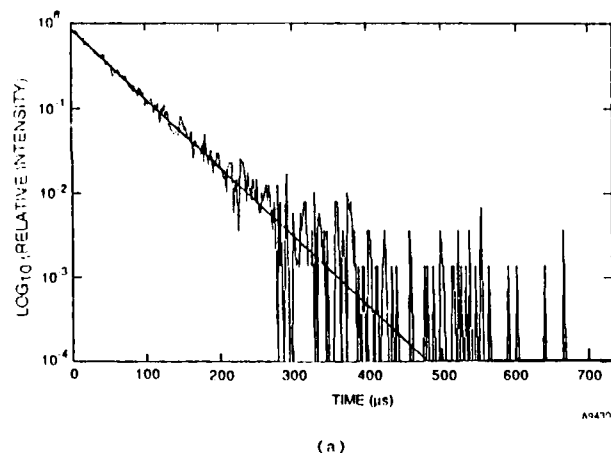


FIG. 3. (a)  $N_2(a, v = 0)$  decay plot for a pressure of 0.9 mTorr. The solid line represents a single decay fit to the data. (b)  $N_2(a)$  decay plot at a pressure of 50 mTorr illustrating the appearance of biexponential relaxation due to coupling with  $N_2(a', v = 0)$ . Note the different time scales.

exponential decay is present. Scattered laser light is detected by the PMT in both traces. Our analysis of the decay rate (solid line fit to the data) begins after the laser signal has decayed (approximately 40  $\mu$ s). The analysis of the data yields values for  $\lambda_1$  or  $\lambda_1$  and  $\lambda_2$ . For biexponential decays the value of  $\lambda_2$  is determined by the diffusion of  $N_2(a')$  ( $\tau_{rad} \sim 20$  ms) out of the detector FOV. A plot of  $\lambda_1$  as a function of  $N_2$  number density is shown in Fig. 4. The slope of this line gives a quenching rate coefficient of  $2.0 \pm 0.1 \times 10^{-11}$  cm<sup>3</sup> molecule<sup>-1</sup> s<sup>-1</sup>. This value is in good agreement with our previous determination of this rate coefficient.<sup>21</sup> The intercept of this plot gives a radiative rate of  $1.78 \pm 0.14 \times 10^4$  s<sup>-1</sup> or a radiative lifetime of  $56.2 \pm 4.6$   $\mu$ s.

This lifetime is somewhat smaller than previous estimates but consistent with Holland's<sup>11</sup> lower limit. Two experiments were performed to confirm the validity of the lifetime measurement. Both experiments were designed to show that transport out of the detector FOV was not a significant contribution to the collisionless  $N_2(a,0)$  loss rate. First, a Hg pen-ray lamp, masked to emit light from only a small pinhole, was scanned across the detector FOV. The detector signal was recorded as a function of light source position. The experiments revealed that the collection efficiency is negligible at the chamber wall. The efficiency rises within 1 cm of the wall to near its maximum value, and then slowly increases by 15% to a maximum in the center of the tank. This variation in efficiency has a very small effect on the measured lifetime.

A second experiment was performed in which an aperture was placed on the PMT to reduce the detector's FOV to a radius of 5 cm at the center of the chamber (factor of 2 reduction). The lifetime measurements were then performed with this restricted FOV. The Stern-Volmer plot of first-order decay rates as a function of  $N_2$  number density for a more restricted set of low-pressure data is shown in Fig. 5. The data give a lifetime of  $58.4 \pm 1.6$   $\mu$ s in good agreement with the expanded FOV measurement. The rate coefficient obtained from the data is  $2.4 \pm 0.2 \times 10^{-11}$  cm<sup>3</sup> molecule<sup>-1</sup> s<sup>-1</sup> (statistical error limits). This rate coefficient is somewhat higher than the value obtained with the full FOV

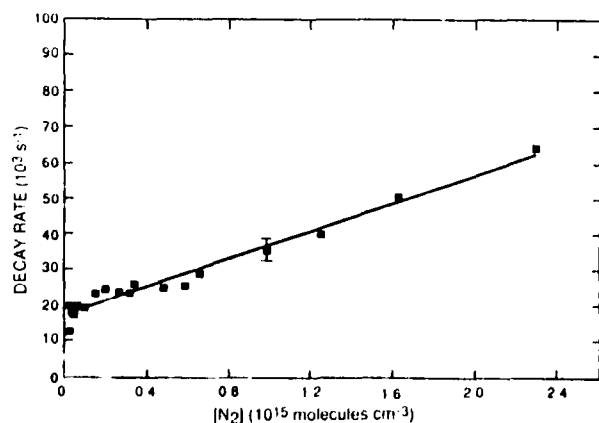


FIG. 4. Plot of  $N_2(a, v=0)$  first-order decay rates ( $\lambda_1$ ) as a function of  $N_2$  pressure. The intercept gives the radiative decay rate ( $\tau = 57.5 \pm 2.3$   $\mu$ s).

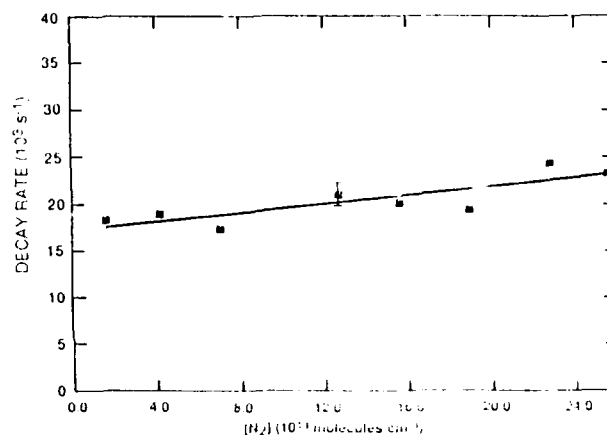


FIG. 5.  $N_2(a, v=0)$  first-order decay rates for the restricted FOV measurement. The intercept gives a radiative lifetime of  $57.4 \pm 1.6$   $\mu$ s.

but is less reliable due to the restricted range of  $N_2$  number densities employed. These two experiments enable us to conclude that FOV effects are not a factor in our lifetime measurements, and provide additional confidence in our results.

## B. Vibrational levels 1 and 2

The Stern-Volmer plot for the relaxation of  $v=1$  is shown in Fig. 6. The lowest pressure radiative decay rates measured in the experiment are nearly identical to those obtained for  $v=0$ . However, at  $N_2$  densities up to  $2 \times 10^{14}$  molecules cm<sup>-3</sup> the apparent decay rate appears to decrease (increasing lifetime) to nearly half the low pressure limit. Similar, though not identical, behavior is observed for the relaxation of  $v=2$  in this pressure range. At higher pressures the relaxation of  $v=1$  appears to proceed at a rate comparable to the rate measured for  $v=0$ . The low pressure behavior observed for  $v=1$  is characteristically obtained in cases where the radiating species diffuses out of the detector field of view. The increase in rate at low pressures occurs in the transition from diffusion controlled to free molecular transport. Our experiments on the lifetime of  $v=0$  effectively preclude this explanation since one would expect virtually identical diffusion coefficients for both vibrational levels.

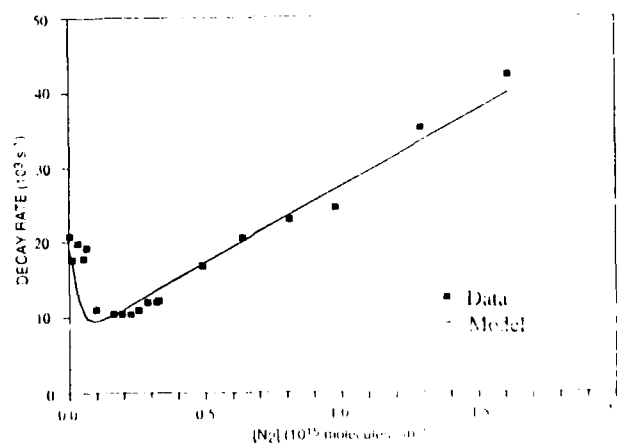


FIG. 6. Stern-Volmer plot for the relaxation of  $N_2(a, v=1)$  by  $N_2$ .

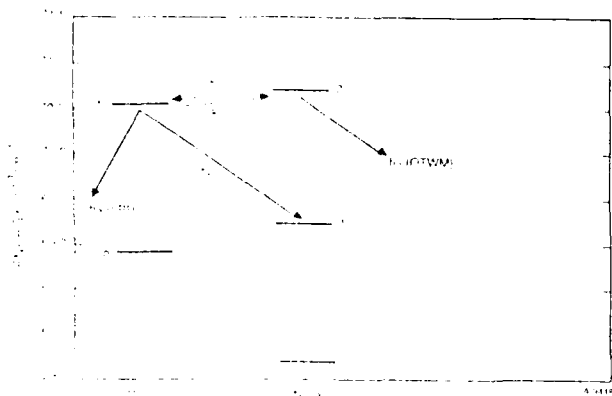


FIG. 7. Energy level diagram for the low-lying levels of  $N_2(a)$  and  $N_2(a')$  illustrating the important processes for the coupling of  $N_2(a, v=1)$  to  $N_2(a', v=2)$ . Radiative decay of the  $a'$  state is through the Ogawa-Tanaka-Wilkinson-Mulliken bands.

We have been able to explain this behavior by considering the effects of coupling of  $N_2(a, v=1)$  to  $N_2(a', v=2)$ . The energy level diagram of Fig. 7 shows the respective energies of the lowest vibrational levels of the  $a$  and  $a'$  states. The lowest vibrational level of the  $a$  state is comparatively isolated. The  $a', v=1$  level lies  $295\text{ cm}^{-1}$  higher in energy (1.5 times  $kT$ ). Hence, coupling of these two levels is less efficient. Our experiments indicate that radiation and quenching to the lower energy  $a', v=0$  level dominate the relaxation process. However,  $v=2$  of the  $a'$  state lies only  $112\text{ cm}^{-1}$  above  $v=1$  of the  $a$  state. Thus, collisional coupling of these levels should be much more facile at 300 K thermal energies. Given the slow loss rate for  $a, v=1$  under higher pressure conditions, it might be expected that, at early times,  $a, v=1$  preferentially couples to  $v=2$  of the  $a'$  state. The reported radiative lifetimes for the  $a'$  state are quite long (several ms),<sup>23,25</sup> hence, this level would simply act as a reservoir state until subsequent collisions can transfer the population back into the  $a$  state. The net result of this process would be an apparent lengthening of the lifetime by the round-trip transit time, which is of course a function of pressure. At higher pressure the two level system becomes completely coupled and the observed decay is that of the coupled system. The important kinetic processes for this mechanism are shown in Fig. 7.

We have constructed a kinetic model of this system in which energy-gap scaling and microscopic reversibility have been employed to describe the coupling of the near-resonant vibrational levels. The degeneracy of each level was obtained by counting all rovibronic states for each level within  $kT$  ( $205\text{ cm}^{-1}$ ) of the vibronic origin and multiplying the sum by the appropriate electronic degeneracy. The rate coefficient for quenching of  $a, v=0$  was used to describe the pure quenching of  $a, v=1$ . The low pressure decay rates were used to define the  $a, v=1$  radiative lifetime. Thus, the model has no adjustable parameters. The rate equations were numerically integrated to obtain the temporal behavior of  $N_2(a, v=1)$ . These decay curves were analyzed using our standard data reduction methods to obtain the first-order

decay rates. The model rates are plotted as the solid curve in Fig. 6. The model shows remarkable agreement with the data. Thus, the near-resonant coupling of the two vibrational manifolds appears to explain the behavior of the first-order decay rates in the single collision pressure regime and we feel justified in using the lowest pressure decay rates to define the radiative lifetime. These radiative lifetimes are  $53.5 \pm 3.8\text{ }\mu\text{s}$  for  $v=1$  and  $51.1 \pm 9.0\text{ }\mu\text{s}$  for  $v=2$ .

## DISCUSSION

The radiative lifetimes for vibrational levels 0–2 reported in this paper represent the first selective and most direct measurements on the  $a^1\Pi_g$  state of  $N_2$ . A laser was employed to excite a specific vibrational level of the  $a$  state and emission from that level was directly observed. In this manner the effects of radiative and collisional cascade were effectively eliminated as a source of error. Our experiments also carefully excluded errors due to field-of-view effects by conducting measurements designed to define the FOV and test the effects of a restricted FOV on the measured result. Finally, the departure of the first-order kinetic decays for  $v=1$  and 2 from idealized Stern-Volmer behavior was explained by coupling to near-resonant levels of the  $a'^1\Sigma_u^-$  state. The radiative lifetimes we have measured for these vibrational levels are indistinguishable, within experimental error. We believe an average value of  $56 \pm 4\text{ }\mu\text{s}$  (two sigma) most accurately reflects the true lifetime.

The shorter radiative lifetime for  $N_2(a)$  measured in this study also has implications for the radiative lifetime of the  $a'^1\Sigma_u^-$  state reported by Piper.<sup>24</sup> In his study the invariance of the  $N_2(a, v=0)/N_2(a', v=0)$  emission intensities with Ar pressure in a discharge flow reactor was used to establish a lower limit on the lifetime of  $a', v=0$ . The steady-state analysis employed gave the following relationship between the lifetimes of  $N_2(a, 0)$  and  $N_2(a', 0)$ :

$$\tau_{a'} \geq \frac{k_1}{k_{-1}} \frac{I_a}{I_{a'}} \tau_a,$$

where  $I_a/I_{a'}$  is the ratio of emission intensities,  $k_1/k_{-1}$  is given by microscopic reversibility, and  $\tau_a$  is the radiative lifetime of  $N_2(a^1\Pi_g, v=0)$ . A critical review of the available literature at the time fixed the  $N_2(a)$  lifetime at  $80^{+40}_{-20}\text{ }\mu\text{s}$ . Hence, Piper was able to place a lower limit of  $23^{+11}_{-6}\text{ ms}$  for the average lifetime of  $a', v=0$ . The lifetime of the forbidden transition is a strong function of rotational level<sup>24</sup> and this value represented an average for a 300 K rotational distribution. Our new value for the  $a$  state lifetime requires that Piper's lower limit be revised to  $17 \pm 2\text{ ms}$ .

The results of the present study can be reconciled with previous measurements of the lifetime by considering the respective measurement techniques which were employed in those studies. The earlier studies were grouped into two classes: the molecular-beam time-of-flight experiments and the curve-of-growth absorption measurements. The fluorescence measurements of Holland<sup>13</sup> and the calculations of Dahl and Oddershede<sup>19</sup> will be discussed separately.

The molecular beam time-of-flight (TOF) studies,<sup>9-12</sup> which comprise the bulk of the measurements, universally discounted the role of the metastable  $a'^1\Sigma_u^-$  state in the col-

TABLE I. Comparison of calculated and measured  $N_2(a^1\Pi_g, v)$  radiative lifetimes.

Vibrational level	$A(a-X)^a$ ( $s^{-1}$ )	$\tau(a-X)$ ( $10^{-6}s$ )	$A(a-a')^b$ ( $s^{-1}$ )	$A(\text{total})$ ( $s^{-1}$ )	$\tau(\text{total})$ ( $10^{-6}s$ )	$\tau(\text{meas.})^c$ ( $10^{-6}s$ )
0	17 062	58.6	100	17 162	56.3	$57.5 \pm 2.3$
1	16 838	59.4	648	17 486	57.2	$53.5 \pm 3.8$
2	16 636	60.1	1186	17 822	56.1	$51.1 \pm 9.0$
3	16 155	61.9	944	17 099	58.5	...
4	14 671	68.2	2169	16 840	59.4	...
Average					$57.9 \pm 2.2$	$56.2 \pm 3.8$

<sup>a</sup> Calculated in Ref. 19.<sup>b</sup> Calculated in Ref. 20.<sup>c</sup> This work.

lision-free decay of metastable  $N_2$ . Freund<sup>26</sup> correctly showed that the collision-free relaxation of these states would be nonexponential due to the radiative coupling of these states via the MacFarlane infrared bands. Our previous paper indicated that the  $a \leftrightarrow a'$  transitions could significantly alter the radiative lifetime of the  $a'$  and, to a lesser extent, the  $a$  state. The particle detectors employed in the TOF measurements could not distinguish between the arrival of near-isoenergetic  $N_2(a)$  and  $N_2(a')$  states. Electron-beam energy threshold measurements were adequate to separate the decay of the longer-lived  $A^3\Sigma_u^+$  state but could not resolve the  $a$  and  $a'$  states. The  $a'$  state was thought to have a much shorter lifetime than current measurements indicate. Hence, it was believed that this state did not contribute to the metastable  $N_2$  flux observed at the detector. A simple analysis of the coupled kinetic decay of this system shows that the combined  $a/a'$  states will appear to decay nonexponentially if followed for several apparent lifetimes. However, most of the TOF experiments did not possess the capability to follow the decay for more than approximately 200  $\mu s$ . Under these conditions the decays appear roughly exponential with apparent lifetimes factors of 1.5 to 4 times the true lifetime. The magnitude of the distortion depends on the relative excitation efficiencies of the two states and the time over which the decay is analyzed. We believe this effect accounts for the wide range of lifetime values, all greater than our current value, reported for this state.

The absorption oscillator strength measurements of the  $a-X$  transition probabilities are somewhat more difficult to analyze. The results of the many studies were surveyed in the introduction. The primary discrepancy in the studies appears to be the ratio of the electric quadrupole to the magnetic dipole contributions ( $Q/D$ ) to the total oscillator strength. Recently, Shemansky<sup>17</sup> has reanalyzed his absorption data to reflect a lifetime closer to the 80  $\mu s$  reported by Holland.<sup>13</sup> The lifetime obtained from Holland's electron beam excitation study was derived from analyzing the spatial extent of the LBH band emission intensity. The 80  $\mu s$  value reported by Holland is actually an upper limit to the lifetime. The observation of nonlinear increases in the populations of some of the low-lying vibrational levels of the  $a$  state led Holland to conclude that additional "slow" cascade mechanisms may be operative. He concluded that the true lifetime may be as short as 40  $\mu s$  if a cascade contribution of 25% to 35% percent is added to the direct production. The

lifetime of 56  $\mu s$  obtained in our studies is consistent with a contribution of that magnitude from the  $a'$  state.

The recent theoretical studies of Dahl and Oddershede<sup>19</sup> are in excellent agreement with our results. They calculated the value of  $Q/D$  to be 0.05; substantially less than determined from the absorption data. These calculations were for the  $a-X$  transition and showed a slight increase in the lifetime over the range from  $v = 0$  to 4. Inclusion of the transition probabilities for the  $a-a'$  transition from our previous paper in the total transition probability reverses the trend in the lifetime data to show a slight decrease, as shown in Table I. The average value of the lifetime for the three lowest levels is  $57 \pm 2 \mu s$  (two sigma). This is well within the range of our experimental uncertainty.

## CONCLUSIONS

Our direct measurement of the radiative lifetime of  $N_2(a, v = 0-2)$  gives an average lifetime of  $56 \pm 4 \mu s$  and is independent of vibrational level, within experimental error. The current results can be rationalized with respect to previous molecular beam time-of-flight and electron beam fluorescence measurements. The data is in excellent agreement with recent theoretical calculations.

## ACKNOWLEDGMENTS

We acknowledge useful discussion with L. G. Piper and G. E. Caledonia of Physical Sciences Inc. This work was supported by the U.S. Air Force Office of Scientific Research under Task 2310G4 and The Defense Nuclear Agency under Project SA, Task SA/SDI, Work Unit 00175.

<sup>1</sup>E. P. Gentieu, P. D. Feldman, and R. R. Meier, *Geophys. Res. Lett.* **6**, 325 (1979).

<sup>2</sup>H. Park, P. D. Feldman, and W. G. Eastie, *Geophys. Res. Lett.* **4**, 41 (1977).

<sup>3</sup>R. E. Hoffman, F. J. LeBlanc, J. C. Larrabee, and D. E. Paulsen, *J. Geophys. Res.* **85**, 2201 (1980).

<sup>4</sup>P. Z. Takaes and P. D. Feldman, *J. Geophys. Res.* **82**, 5011 (1977).

<sup>5</sup>G. J. Rottman, P. D. Feldman, and H. W. Moos, *J. Geophys. Res.* **78**, 258 (1973).

<sup>6</sup>F. Paresce, M. Lumpton, and J. Holberg, *J. Geophys. Res.* **77**, 4773 (1972).

<sup>7</sup>A. Lofthus and P. H. Krupenie, *J. Phys. Chem. Ref. Data* **6**, 113 (1977).

<sup>8</sup>R. A. McFarlane, *J. Quantum Electron.* **2**, 229 (1966).

<sup>9</sup>W. Lichten, *J. Chem. Phys.* **26**, 306 (1957).

- <sup>17</sup>J. Olmsted III, A. S. Newton, and K. Street, Jr., *J. Chem. Phys.* **42**, 2321 (1965).
- <sup>18</sup>W. I. Borst and E. C. Zipf, *Phys. Rev. A* **3**, 979 (1971).
- <sup>19</sup>N. J. Mason and W. R. Newell, *J. Phys. B At. Mol. Phys.* **20**, 3913 (1987).
- <sup>20</sup>R. F. Holland, *J. Chem. Phys.* **51**, 3940 (1969).
- <sup>21</sup>R. H. Garstang, *J. Chem. Phys.* **44**, 1308 (1966).
- <sup>22</sup>B. K. Ching, G. R. Cook, and R. A. Becker, *J. Quant. Spectrosc. Radiat. Transfer* **7**, 323 (1967).
- <sup>23</sup>D. E. Shemansky, *J. Chem. Phys.* **51**, 5487 (1969).
- <sup>24</sup>J. M. Aiello and D. E. Shemansky, *J. Geophys. Res.* **90**, 9845 (1985).
- <sup>25</sup>M. J. Pilling, A. M. Biss, and W. Braun, *J. Quant. Spectrosc. Radiat. Transfer* **11**, 1593 (1971).
- <sup>26</sup>F. Dahl and J. Oddershede, *Phys. Scr.* **33**, 135 (1986).
- <sup>27</sup>W. J. Marinelli, B. D. Green, M. A. DeFaccio, and W. A. M. Blumberg, *J. Phys. Chem.* **92**, 3429 (1988).
- <sup>28</sup>W. J. Marinelli, W. J. Kessler, B. D. Green, and W. A. M. Blumberg, *J. Chem. Phys.* **90**, 2167 (1989).
- <sup>29</sup>P. B. Sackett, *Appl. Opt.* **11**, 2181 (1972).
- <sup>30</sup>M. P. Casassa and M. F. Golde, *Chem. Phys. Lett.* **60**, 281 (1979).
- <sup>31</sup>S. G. Tilford and W. M. Benesch, *J. Chem. Phys.* **64**, 3370 (1976).
- <sup>32</sup>L. G. Piper, *J. Chem. Phys.* **87**, 1625 (1987).
- <sup>33</sup>R. S. Freund, *J. Chem. Phys.* **56**, 4344 (1972).



Accession For	
NTIS (CR42)	<input checked="" type="checkbox"/>
DTIC TAB	<input type="checkbox"/>
Unannounced	<input type="checkbox"/>
Justification	
By	
Distribution/	
Availability Codes	
Dist	Avail and/or Special
A-1	20